Biomedicine & Pharmacotherapy 152 (2022) 113209

Contents lists available at ScienceDirect

Biomedicine & Pharmacotherapy

journal homepage: www.elsevier.com/locate/biopha

# Extracellular vesicles of cannabis with high CBD content induce anticancer signaling in human hepatocellular carcinoma

Tahereh Tajik [a,b], Kaveh Baghaei [b,c,*,1], Vahid Erfani Moghadam [d,e,**,2], Naser Farrokhi [a,***,3], Seyed Alireza Salami [f,g]

[a] Faculty of Life Sciences and Biotechnology, Shahid Beheshti University, Tehran, Iran
[b] Basic and Molecular Epidemiology of Gastrointestinal Disorders Research Center, Research Institute for Gastroenterology and Liver Diseases, Shahid Beheshti University of Medical Sciences, Tehran 1985717413, Iran
[c] Gastroenterology and Liver Diseases Research center, Research Institute for Gastroenterology and Liver Diseases, Shahid Beheshti University of Medical Sciences, Tehran 1985717413, Iran
[d] Department of Medical Nanotechnology, School of Advanced Technologies in Medicine, Golestan University of Medical Sciences, Gorgan, Iran
[e] Food, Drug, Natural Products Health Research Centre, Golestan University of Medical Science, Gorgan, Iran
[f] Department of Horticultural Science, Faculty of Agricultural Sciences and Engineering, University of Tehran, Karaj, Iran
[g] Industrial and Medical Cannabis Research Institute (IMCRI), Tehran 14176-14411, Iran

ARTICLE INFO

*Keywords:*
Apoptosis
Cannabidiol
Phytocannabinoids
Cell cycle arrest
Extracellular vesicles

ABSTRACT

Plant-derived extracellular vesicles (EVs) have been the topic of interest in recent years due to their proven therapeutic properties. Intact or manipulated plant EVs have shown antioxidant, anti-inflammatory, and anti-cancerous activities as a result of containing bioactive metabolites and other endogenous molecules. Less is known about the EV efficacy with high levels of bioactive secondary metabolites derived from medicinal or non-edible plants. Numerous data suggest the functionality of *Cannabis sativa* extract and its phytocannabinoids in cancer treatment. Here, two chemotypes of cannabis with different levels of D-9-tetrahydrocannabinol (THC) and cannabidiol (CBD) were selected. EVs were isolated from each chemotype via differential ultracentrifugation. HPLC analysis was illustrative of the absence of THC in EVs derived from both plants. Therefore, two types of EVs were classified according to their CBD content into high- (H.C-EVs) and low-CBD EVs (L.C-EVs). Electron microscopy and DLS showed both cannabis-derived EVs (CDEVs) can be considered as exosome-like nanovesicles. Cytotoxicity assay showed that H.C-EVs strongly decreased the viability of two hepatocellular carcinoma (HCC) cell lines, HepG2 and Huh-7, in a dose and time-dependent manner compared with L.C-EVs. H.C-EVs had no significant effect on HUVECs normal cell growth. The finding showed that the H.C-EVs arrested the G0/G1 phase in the cell cycle and significantly induced cell death by activating mitochondrial-dependent apoptosis signaling pathways in both HCC cell lines. Altogether, the current study highlights that CDEVs can be an ideal natural vehicle for bioactive phytocannabinoids and a promising strategy in cancer management.

*Abbreviations:* BAX, BCL2 associated X; Bcl-xl, BCL-2-like 1 isoform Bcl-X(L); CASP3, caspase-3; CASP8, caspase-8; CASP9, caspase-9; CBD, cannabidiol; CDEVs, cannabis-derived extracellular vesicles; EVs, extracellular vesicles; GAPDH, glyceraldehyde-3-phosphate dehydrogenase; HCC, hepatocellular carcinoma; H.C-EVs, high-CBD EVs; L.C-EVs, low-CBD EVs; MVBs, multivesicular bodies; THC, D-9-tetrahydrocannabinol.

* Corresponding author at: Basic and Molecular Epidemiology of Gastrointestinal Disorders Research Center, Research Institute for Gastroenterology and Liver Diseases, Shahid Beheshti University of Medical Sciences, Tehran 1985717413, Iran.
** Corresponding author at: Department of Medical Nanotechnology, School of Advanced Technologies in Medicine, Golestan University of Medical Sciences, Gorgan, Iran.
*** Corresponding author.
*E-mail addresses:* vahid.erfani@goums.ac.ir (K. Baghaei), kavehbaghai@gmail.com (V.E. Moghadam), n_farrokhi@sbu.ac.ir (N. Farrokhi).
[1] ORCID: 0000-0003-2102-9729.
[2] ORCID: 0000-0002-6723-5766.
[3] ORCID: 0000-0003-4676-1545.

https://doi.org/10.1016/j.biopha.2022.113209
Received 22 March 2022; Received in revised form 24 May 2022; Accepted 25 May 2022
Available online 3 June 2022

## 1. Introduction

The discovery of extracellular vesicles in the 1950s opened new insights into the understanding of intercellular, inter-species, and inter-kingdom communications [1,2]. EVs, nano-sized bilayer lipid vesicles, are being released from different cell types and can be classified into subgroups, namely apoptotic bodies, microvesicles, and exosomes, according to their origin and size [3]. Apoptotic bodies (1000–5000 nm) are being generated from the cells that undergo apoptosis, to be phagocytosed. Microvesicles are being originated from phospholipid membrane with a size range of 150–1000 nm. Exosomes with 30–150 nm in size are being derived from multi-vesicular bodies (MVBs) [2]. Naturally, EVs transfer endogenous molecules as cargo to recipient cells [4]. In EV-based therapeutics, molecules such as siRNA, microRNA, as well chemicals, and biological drugs have been encapsulated within these vehicles to be delivered to the targets of interest [5–7]. Exosomes have been considered as the promising biomarkers in the early diagnosis of diseases such as infectious diseases, autoimmune disorders, diabetes, and several types of cancers [2,8–10]. Recently, large-scale production of EVs from edible and herbal plants (range in size, 30–500 nm) has been noticed as an excellent source of nanovesicles with phenomenal intrinsic properties and known minimal side-effects [11,12].

The presence of small vesicles derived from MVBs in the apoplastic milieu of plant cells has been demonstrated in several independent microscopic studies [13–15]. Plant-derived EVs are similar to mammalian exosomes in structure and density with roles in interspecies communication such as pathogen-host interactions, non-canonical proteins secretion, and subsequently cell wall remodeling [16–19]. A distinctive feature of plant-derived versus animal EVs is their inner secondary metabolites content and some other phytocompounds that can potentially be therapeutic [20,21]. In fact, without the need to load drugs or exogenous molecules into plant EVs, they inherently show natural therapeutic benefits [22]. Thus, they can be a novel treasure for the discovery of innovative treatment strategies [23,24]. Additionally, it has been shown that plant-derived EVs have the ability to target specific tissues and can be used as inexpensive and safe carriers for the delivery of drugs and genetic material in nanomedicine [22,25]. Over the past several years, intact or manipulated plant EVs have shown their potential as antioxidant [24], anti-inflammatory [26], anti-melanogenic [27], and anti-cancerous [28] agents. The latter has been reported in the inhibition of several cancer cell lines. EVs isolated from lemon juice have been reported to exert anti-proliferative and anticancer activities on gastric cancer in both in vitro and in vivo models [29]. In another study, isolated EVs from four types of plant sap have shown selective antitumor effects [30]. These anticancer properties show the importance of some plant EVs in the horizon of novel pharmaceutical technologies for cancer treatment.

*Cannabis sativa* L. is a mysterious and multi-purpose plant from Cannabaceae that has been used as fiber, food, oil, and herbal remedy since time immemorial [31]. Cannabis contains unique phytochemicals such as phytocannabinoids, triterpenes, sesquiterpenes, and flavonoids [32]. Phytocannabinoids are lipophilic ligands for cannabinoid receptors (CB) on the surface of specific human cells, thus can activate different signaling pathways [33,34]. D-9-tetrahydrocannabinol (THC) and cannabidiol (CBD) are the two important members of the phytocannabinoids family [35]. Based on their concentration, cannabis has been classified into drug-type (high amount of THC) or hemp-type (high amount of CBD) [32]. In another classification, five chemotypes (chemical phenotypes) of cannabis are defined based on the composition of phytocannabinoids (especially THC and CBD), ratios, and their quantities [31]. Each chemotype has a unique function due to varying concentrations of its cannabinoids [33]. Cannabis extract and some of its phytocannabinoids, such as THC and CBD, have been demonstrated to exert anti-proliferative and anticancer activities [36–39]. Various mechanisms are proposed for the actions behind THC and CBD anticancer activities, including cell cycle arrest and inhibition of proliferation, induction of autophagy and apoptosis, inhibition of adhesion, migration, angiogenesis, and metastasis [40,41]. Moreover, in several cancer cell lines role of CBD as an inhibitor or modulator of biogenesis and release of EVs has been reported. Therefore, the use of CBD may increase the susceptibility of these cancers to chemotherapy [42,43]. To the best of our knowledge, the effects of extracellular vesicles derived from the cannabis plant on various cancer cell lines have not been addressed so far.

Hepatocellular carcinoma (HCC) is the major form of primary liver cancer and a serious threat to human health [44]. HCC is considered the third leading cause of cancer-related mortality and the sixth most common cancer globally [45,46]. HCC incidence has been growing on a global scale and is expected to increase until 2030 [47]. The high and growing incidence of HCC is mainly due to the increasing prevalence of hepatitis types B and C, obesity, diabetes, alcohol consumption, aflatoxin exposure, and smoking [48]. The proliferative capability of HCC cells is very high [47,49]. Due to the late diagnosis in the vast majority of HCC patients, chemotherapy is the method of choice for cancer therapy and bringing the cell proliferation to halt [44]. It has been shown that the induction of apoptosis can destroy cancer cells and reduce their proliferation rate [50]. Thus, the design of novel therapeutic strategies to successfully target genes involved in apoptosis may promise more efficient ways of HCC management.

In the current study, by building on the determined anticancer properties of cannabis extract and its cannabinoids [36], the feasibility of isolating EVs from two *Cannabis sativa* chemotypes (Ark-01: CBD-predominant chemotypes, and Krmn-01: THC-predominant chemotypes) [51] was assessed for the first time (noted as cannabis-derived extracellular vesicles (CDEVs) henceforth). Furthermore, their possible anticancer effects were examined on two hepatocellular cancer cell lines as a new research field in cancer therapy.

## 2. Materials and methods

### 2.1. Plant material and isolation of CDEVs by differential ultracentrifugation

Two chemotypes of the cannabis plant (**Ark-01** and **Krmn-01**) were obtained from the Center for Genetic Resources of Cannabis, Iran (CGRC; www.medcannabase.org), Tehran University Research Farm, Karaj, Iran. For isolation of CDEVs, female inflorescences of two cannabis chemotypes were used. The fresh inflorescences were washed twice with $dH_2O$ at 22 °C and 20 g of them (flowers without woody parts) were homogenized three times [1 min each with 30 s intervals] in 200 ml phosphate-buffered saline (PBS, 4 °C) using a homogenizer (Witeg Wisd, Germany). The plant homogenized material was sequentially centrifuged (Eppendorf, Germany) at 1000×*g* and 3000×*g* for 30 min each to remove the large particles and debris. The EVs-enriched solution was collected from the supernatant following centrifugation at 10,000×*g* for 1 h. The supernatant was filtered through a 0.45 μm filter and ultra-centrifuged at 120,000×*g* for 90 min using an SW28 Beckman rotor (Beckman Coulter, USA). The pellets were washed and suspended in 1–2 ml PBS (depending on the yield) and transferred to a sucrose density gradient column (cushions of 8 %, 15 %, 30 %, 45 %, and 60 % w/v) and centrifuged at 120,000×*g* for 120 min. The sucrose gradient ultra-centrifugation was performed to further purify isolated EVs from proteins, RNAs, and other vesicles deposited in the previous step. All centrifugation steps were carried out at 4 °C. The bands between the 30–45 % layers were harvested (as the best source of plant exosome-like nanovesicles) [12] and placed at PBS. The suspension was centrifuged at 120,000×*g* for 90 min. The pellets were suspended in PBS and were stored at − 70 °C (Fig. 1).

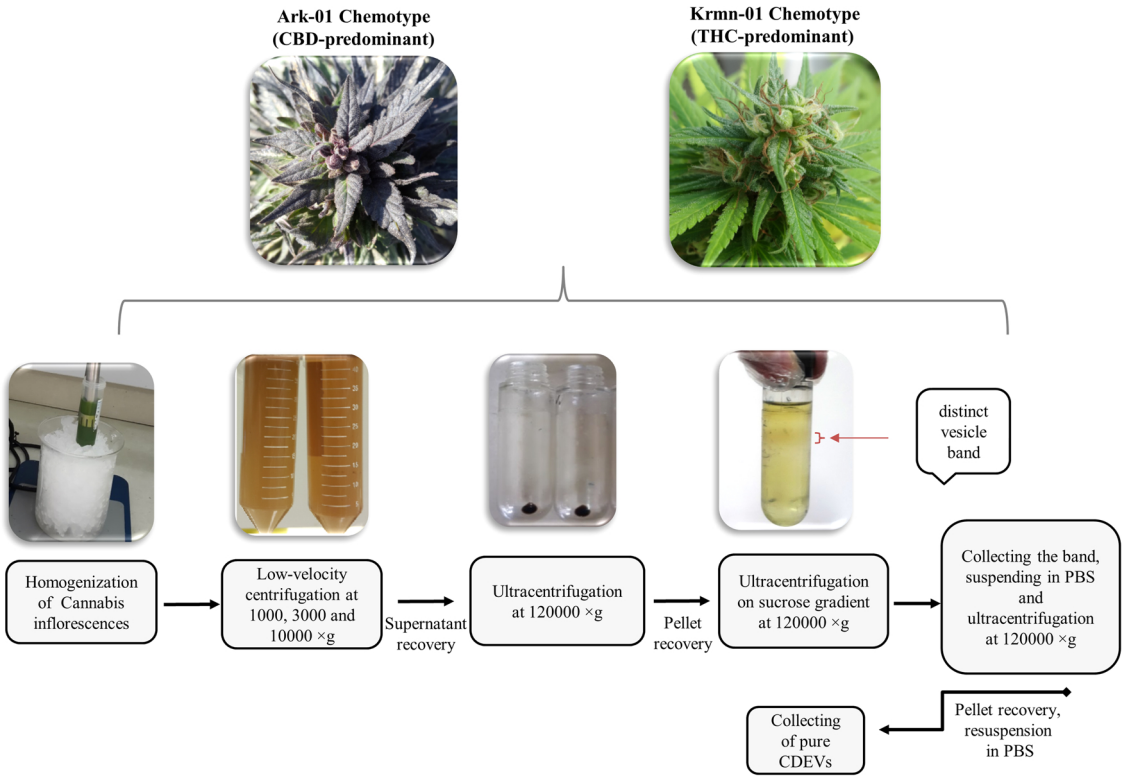


**Fig. 1.** Experimental workflow for describing the isolation method of cannabis-derived extracellular vesicles (CDEVs) from two chemotypes (Ark-01; CBD-predominant chemotype and Krmn-01; THC-predominant chemotype). Homogenized flowers were purified from debris and large particles by a series of low-velocity centrifugation and supernatant recovered. Finally, CDEVs were isolated by ultra-centrifugation coupled with a sucrose density gradient.

### *2.2. Characterizations of CDEVs*

#### *2.2.1. BCA protein assay*

Protein concentration was used as an estimate of EV yield in each preparation run. Total protein concentration was measured by a micro BCA assay kit (DNABioTech, Tehran, Iran) according to the manufacturer's instruction. In brief, 25 μl of CDEVs were mixed with 75 μl BCA working solution in a microtube with a buffer-only sample as the control and BSA standard (0.003–1 μg/μl). The samples were incubated at 60 °C for 1 h and cooled at 22 °C. After brief vortex mixing, 100 μl of each sample was transferred to a 96-well microplate and $OD_{562}$ in a microplate reader (Epoch, BioTek, USA) was measured. A standard curve was plotted to convert $OD_{562}$ to protein concentration.

#### *2.2.2. CDEVs size determination*

The hydrodynamic size distribution of CDEVs was distinguished using the dynamic light scattering (DLS) method. The collected CDEVs (30 μl) were diluted in 1 ml of PBS and placed in a cuvette for analysis at 20 °C. Determining size distribution of CDEVs was performed on the Zetasizer Nano ZS90 system (Malvern Instrument, UK) in triplicate.

#### *2.2.3. Transmission Electron Microscopy (TEM)*

The morphological evaluation of the isolated CDEVs was performed by Zeiss Leo 906 TEM (Carl Zeiss, Oberkochen, Germany). Briefly, a drop of each CDEVs sample was loaded onto 300 mesh formvar-carbon-coated copper grids and incubated for 5 min. Excess fluid was carefully removed with filter paper and grids negatively stained with 2 % (w/v) uranyl acetate for 3 min. The grids were air-dried and TEM imaging was recorded.

#### *2.2.4. Field Emission-Scanning Electron Microscopy (FE-SEM)*

For identification of EVs morphology and size, as well as discrimination from the other particles, FE-SEM (TESCAN MIRA3-XMU, Czechia) was applied at 15.0 kV. The CDEVs were fixed with 3.7 % glutaraldehyde in PBS for 24 h at 4 °C. The samples were washed with PBS for 5 min and dehydrated in an ethanol dilution series (50 %, 60 %, 70 %, 80 %, 90 %, and 99 %) for 10 min each. The samples were air-dried for 24 h, coated with Platinum, and observed by FE-SEM instrument.

### *2.3. THC and CBD content analysis*

Dried cannabis flowers (5 g) from two chemotypes were separately ground to fine powder and 50 mg were used for THC and CBD content analysis via HPLC. In addition to the raw plant material, 5 mg of lyophilized CDEVs were used for the same purpose. Methanol: chloroform (1.5 ml of 9:1 v/v) was added to both tubes containing powdered florets and CDEVs, and vortexed for 5 min. Extraction took place using a sonication bath for 40 min where samples were mixed using a vortex every 20 min. The tubes were centrifuged at 10,000 rpm for 15 min to remove the large particles and debris. Supernatants were transferred to new micro-tubes and air-dried at 22 °C. Methanol (1 ml) was added to each tube and centrifuged at 13,000 rpm for 10 min. Supernatants were harvested and stored at 4 °C until HPLC analysis.

Smartline model system (Knauer, Germany) equipped with a diode-array detector UV–VIS (DAD)− 2800, and a reversed-phase C18 column protected by a KNAUER guard column and pre-column (MZ Cartridges 10 mm) was used for HPLC. The separation was carried out using an isocratic flow. The mobile phase was a mixture of $dH_2O$: methanol (2:8 v/v; Merck KGaA, Darmstadt, Germany). The analyses with an injection volume of 20 μl were conducted at 30 °C with a 1 ml/min flow rate. Peaks of cannabinoids were monitored at 220 nm. Calibration curves were plotted using standard solutions containing 0.1 mg/ml of THC and CBD (Sigma Aldrich, USD; TK#61–65 and TK#61–477, respectively). Data were processed by ChromGate Software (V 3.1.7).

### 2.4. Cell culture

Two human liver cancer cell lines, HepG2 and Huh-7 (hepatic carcinoma cells), were obtained from the Pasteur Institute of Iran (Tehran, Iran). Non-cancer cell line, HUVECs (Human umbilical vein endothelial cells), was donated by the research institute for gastroenterology and liver diseases (Tehran, Iran). The Huh-7 and HUVECs cells were cultured in DMEM medium (Biosera, Iran). The HepG2 cells were grown in DMEM-F12 medium. Both culture media were enriched with 10 % fetal bovine serum (FBS; Gibco, Paisley, UK) plus 1 % penicillin/streptomycin (100 U/ml of penicillin and 100 mg/ml streptomycin) (Gibco, Paisley, UK). The cells were maintained at 37 °C in a humidified atmosphere with 5 % $CO_2$. Experiments were carried out when cells were in an exponential growth stage.

### 2.5. MTT assay

The viability of HepG2 and Huh7 cancer cells and HUVECs normal cells were measured using MTT (3-(4,5-dimethylthiazol-2-yl)−2, 5-diphenyltetrazolium bromide) assay to evaluate cytotoxicity effects of H.C-EVs and L.C-EVs. Briefly, the cells were seeded in 96-well plates ($1 \times 10^4$ cells/well of HepG2 and $5 \times 10^3$ cells/well of Huh7 and HUVECs) for 24 h. The cells were exposed to 0, 25, 50, 100, 150, and 200 μg/ml CDEVs (expressed as protein content) in 200 μl full medium for 24 and 48 h. Following incubation at 37 °C, the medium was removed, and 100 μl of culture medium containing MTT solution (5 mg/ml, Sigma, USA) was added to each well and incubated at dark for 4 h. MTT solution was removed and formazan crystals were dissolved by 100 μl dimethyl sulfoxide (Sigma, St. Louis, USA) and the absorbance was checked at 570 nm by a microplate reader (Epoch, BioTek, USA). Cell viability diagrams were generated from at least three independent experiments with three technical replicates per plate and plotted as the percentage of growth versus control (untreated cells).

### 2.6. Apoptosis detection by flow cytometry

Cell apoptosis assay was conducted by Annexin V/PI Apoptosis Detection Kit (BioLegend, San Diego, CA, USA) according to the manufacturer's instruction. Briefly, HepG2 and Huh-7 cells were treated with 100 and 150 μg/ml of H.C-EVs and L.C-EVs. Cells were harvested, washed twice with cold PBS, and resuspended in 100 μl of Annexin V binding buffer. The cells' density of the suspension was adjusted to $0.5–1.0 \times 10^6$ cells/ml. The cell suspension was transferred in a 5-ml test tube. FITC Annexin V (5 μl) and 10 μl of propidium iodide (PI) solution were added to the cells of each tube. The tubes were vortexed and incubated for 15 min at 22 °C at dark. Annexin V binding buffer (400 μl) was added to each tube and immediately subjected to flow cytometer (FACSCalibur, BD Biosciences, San Jose, CA, USA) using a 488 nm laser. The apoptotic rates of cells were analyzed by flowjo software (version 7.6.1; FlowJo, LLC, Ashland, OR, USA).

### 2.7. Cell cycle analysis

The cell cycle distribution of HepG2 and Huh-7 cells was determined following treatment with H.C-EVs and L.C-EVs by flow cytometry. For this assay, HepG2 and Huh-7 cells were seeded in a six-well plate for 24 h and exposed to 150 μg/ml H.C-EVs and L.C-EVs. After incubation, cells were harvested, washed with cold PBS, and fixed in 500 μl 70 % ice-cold ethanol at 4 °C for 2 h. The cells were centrifuged at 300*g* for 5 min and washed twice with PBS +2 % FBS to remove the ethanol. The cells were treated with 50 μl of RNase A (100 μg/ml) (DNAbioTech, Tehran, Iran) and incubated at 37 °C for 30 min. The cells were subjected to 150 μl of staining buffer cocktail containing propidium iodide (50 μg/ml) (Sigma-Aldrich, Irvine, UK), Triton X-100 (Sigma-Aldrich, Irvine, UK), and PBS buffer for 30 min at 4 °C while protected from light. A minimum of 10,000 stained cells per sample was counted using a flow cytometer (FACSCalibur, BD Biosciences, USA). Percentages of cells in G0/G1, S, and G2/M phases were measured using flowJo software (version 7.6.1; FlowJo, LLC, Ashland, OR, USA).

### 2.8. Quantitative real-time PCR (qRT-PCR)

Total RNA was isolated from HepG2 and Huh-7 cells after treatment with H.C-EVs at a concentration lower than their respective $IC_{50}$, using a total RNA isolation kit (Yekta Tajhiz Azma, Tehran, Iran) according to the manufacturer's instructions. Complementary DNA (cDNA) was synthesized from 0.5 μg total RNA per sample using random hexamer primers and a cDNA synthesis kit (Yekta Tajhiz Azma, Tehran, Iran). Quantitative real-time PCR reactions were performed in a 20 μl volume by applying SYBR Green Master Mix (Yekta Tajhiz, Tehran, Iran) and a Rotor-Gene Q real-time PCR system (Qiagen, Hamburg, Germany) under the following three-step cycling: initial denaturation for 5 min at 95 °C, followed by 40 cycles of 95 °C: 10 s; 59 °C: 20 s; 72 °C: 20 s. To investigate any spurious amplification products, melting curves were generated from 70 to 95 °C. The expression level of each gene was normalized using the detection of *GAPDH* as an internal control for mRNA and calculated by the $2^{-\Delta\Delta Ct}$ method [52]. Each experiment was repeated three times. The sequences of all the primers are listed in Table 1, which was designed using the NCBI Primer-Blast Tools and OLIGO v.7.56 software (Molecular Biology Insights, Inc., USA).

### 2.9. Statistical analysis

Each assay was carried out in three independent experiments with at least three replicates and data expressed as means ± standard deviation (SD). Results were analyzed using GraphPad Prism v.8.4.3 software (GraphPad, La Jolla, CA, USA). Statistical significance between two groups was calculated using unpaired Student's t-test. One-way analysis of variance (ANOVA) was performed to compare between different groups. Differences were considered statistically significant when *P*-values were less than 0.05 levels ($p < 0.05$).

## 3. Results

### 3.1. Isolation and characterization of CDEVs

Cannabis female inflorescence is typically used for pharmacological purposes due to the abundance of important metabolites (i.e. cannabinoids) in trichomes of female flowers. CDEVs were isolated from two cannabis chemotypes **(Ark-01; CBD**-pre**dominant** chemotype and **Krmn-01; THC-predominant** chemotype) **by** differential ultra-centrifugation **method** coupled with a sucrose density gradient **(**Fig. 1**)**. To confirm the successful isolation of the EVs, the size and morphology of the ultra-centrifugation products were investigated. DLS results showed that the size distribution of EVs isolated from **Ark-01chemotype** ranged from 37.84 to 255.0 nm, with an average diameter of 163.9 ± 27.16 nm. EVs isolated from **the Krmn-01** chemotype

**Table 1**
Primers designed and used in quantitative real-time PCR.

| Name | Sequence (5'→3') | Amplicon size (bp) |
|---|---|---|
| CASP3 | Fw: AAGCGAATCAATGGACTCTGG<br>Rv: GACCGAGATGTCATTCCAGTG | 123 |
| CASP9 | Fw: AACAGGCAAGCAGCAAAGT<br>Rv: TCCTCCAGAACCAATGTCCA | 132 |
| CASP8 | Fw: AGGAATGGAACACACTTGGATG<br>Rv: GAGAGGATACAGCAGATGAAGC | 170 |
| BAX | Fw: AGGTCTTTTTCCGAGTGGCA<br>Rv: GAGGAAGTCCAATGTCCAGC | 164 |
| Bcl-xl | Fw: ACTGTGCGTGGAAAGCGTAG<br>Rv: AAAGTATC'CCAGCCGCCGTT | 126 |
| GAPDH | Fw: TTGCCCTCAACGACCACTTT<br>Rv: TGGTCCAGGGGTCTTACTCC | 120 |

had a size distribution range of 32.67–220.2 nm, with an average size of 133.2 ± 5.75 nm (Fig. 2A). DLS data were confirmed by FE-SEM images that revealed both CDEVs had a uniform size distribution (Fig. 2B). The morphology and integrity of vesicles were visualized using TEM. TEM images showed that two CDEVs samples were generally spherical or oval-shaped with an intact bilayer membrane (Fig. 2B). Altogether, based on electron microscopy examinations and DLS analysis, the CDEVs were distinguishable as exosome-like nanovesicles.

### 3.2. CBD and THC contents of CDEVs

CBD and THC contents were analyzed by HPLC in both cannabis extracts and CDEVs. HPLC data showed that EVs derived from two cannabis chemotypes carried different proportions of CBD and THC compared to the plant of CDEV origin. Interestingly, EVs isolated from Ark-01chemotype, similar to the plant of origin, contained a high concentration of CBD (1.46 ± 0.2 μg/mg) whereas in EVs isolated from Krmn-01 chemotype, unlike the maternal plant, no THC was detected and the accumulation of CBD was about half that of Ark-01-derived EVs (0.75 ± 0.25 μg/mg). Therefore, EVs isolated from Ark-01 and Krmn-01 chemotypes were called High-CBD EVs (H.C-EVs) and low-CBD EVs (L.C-EVS), respectively (Fig. 3).

### 3.3. Efficacy of CDEVs on the viability of HCC cells

To study the effect of CDEVs on HCC cells viability, an MTT assay was performed. HepG2 and Huh-7 cells were incubated with different concentrations of H.C-EVs and L.C-EVs for 24 and 48 h. Both types of CDEVs negatively influenced the viability of the two liver cancer cell lines, albeit to a different extent (Fig. 4). The results showed that the viability percentage of HepG2 and Huh-7 cells treated with H.C-EVs were clearly decreased compared to the control (untreated cells) in a time and concentration-dependent manner (Fig. 4A-B). The cytotoxic effect of H.C-EVs was detectable at a concentration of 25 μg/ml after 24 h on both cancer cell lines. Additionally, a 50 % growth reduction in HepG2 cells was observed following treatment with 100 μg/ml of H.C-EVs after 48 h. As for Huh-7 cells, the viability reached less than 50 % after exposure to 150 μg/ml of H.C-EVs for 24 h. Following the concentration increase, the L.C-EVs gradually reduced the viability of both cell lines, while their cytotoxicity effect was significantly very lower than H.C-EVs. These EVs reduced viability of both HepG2 and Huh-7 cell lines by less than 25 %. According to the results of this assay, H.C-EVs showed more anti-cancer activity compared to L.C-EVs on two.

cancer cell lines. Accordingly, H.C-EVs (five concentrations) were used to treat HUVECs cells for 24 and 48 h, to assess its effects on a normal cell line (Fig. 4C). Interestingly, no potential cytotoxic effect was evident on HUVECs cells at 24 and 48 h after treatment and their viability remained statistically unchanged. The viability percentage of HUVECs cells treated with H.C-EVs was maintained more than 88 %, even after treatment with the highest concentration of the corresponding EVs (200 μg/ml). Among five concentrations used of H.C-EVs and L.C-EVs in the MTT assay, the concentrations of 100 and 150 μg/ml and incubation times of 24 h for the Huh-7 cell line and 48 h for the HepG2 cell line (which best cellular responses were obtained at these incubation times) were selected for conducting the subsequent analyses.

### 3.4. Role of CDEVs on HCC apoptosis

To investigate whether the CDEVs' inhibitory effects on HCC cells viability are related to the induction of apoptosis, the Annexin V-FITC/PI method was performed that followed by flow cytometry. Flow cytometry results indicated that increasing concentrations of H.C-EVs (from 100 to 150 μg/ml) results in a significant increase in apoptotic cells percentage (the sum of the early and late apoptosis) in HepG2 and Huh-7 cells compared to untreated cells (Figs. 5 and 6). The rate of apoptosis in HepG2 cells strongly increased from 4.68 ± 2.33 % in the untreated cells to 36.21 ± 4.17 % ($p < 0.001$) and 46.26 ± 7.76 % ($p < 0.0001$) following treatment with 100 and 150 μg/ml H.C-EVs, respectively (Fig. 5 A and B). Furthermore, the apoptosis percentage of Huh-7 cells significantly altered from 6.52 ± 3.32 % in the untreated cells to 27.99 ± 6.43 % ($p < 0.01$) and 39.4 ± 3.61 % ($p < 0.001$) in the concentrations of 100 and 150 μg/ml H.C-EVs, respectively (Fig. 6A and

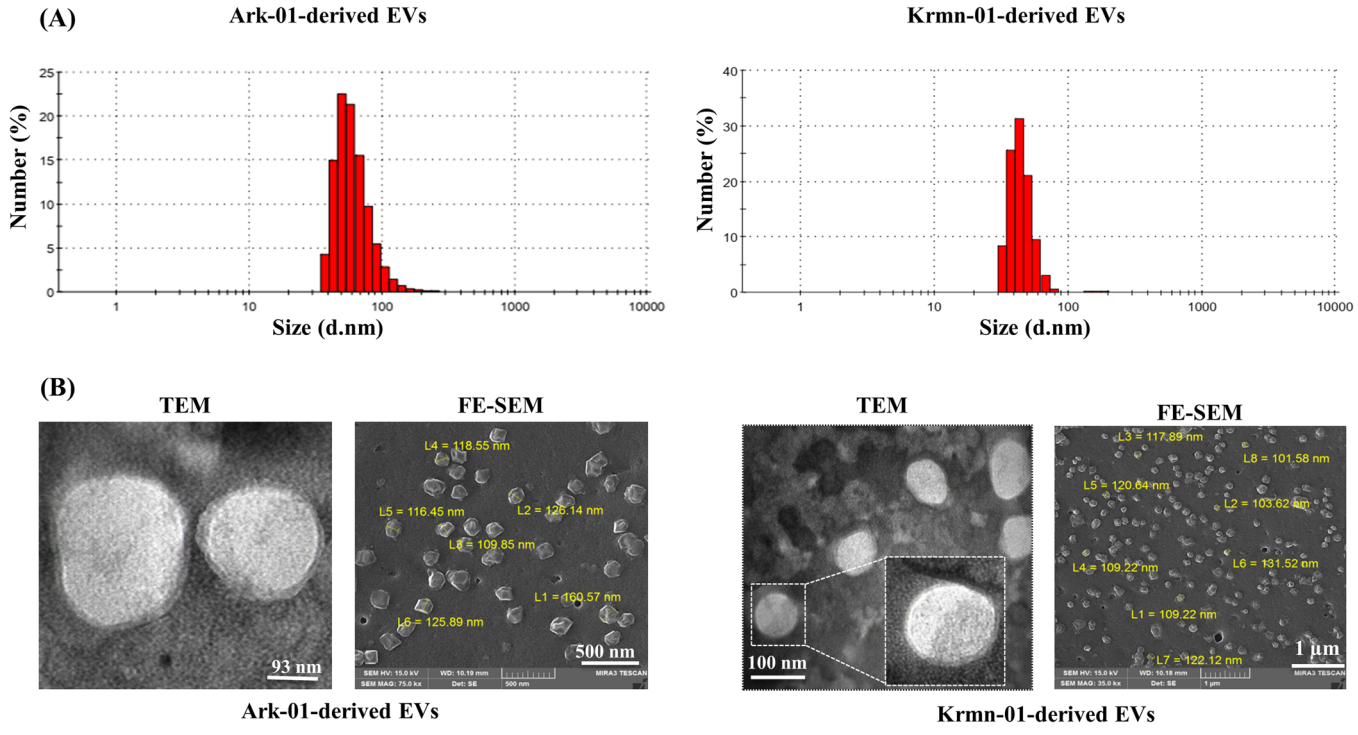


**Fig. 2.** Characterization of EVs derived from two cannabis chemotypes (Ark-01and Krmn-01). (A) Size distributions of EVs isolated of Ark-01and Krmn-01chemotype were determined using Malvern Zeta analyzer. (B) TEM and FE-SEM images of Ark-01-derived EVs and Krmn-01-derived EVs.

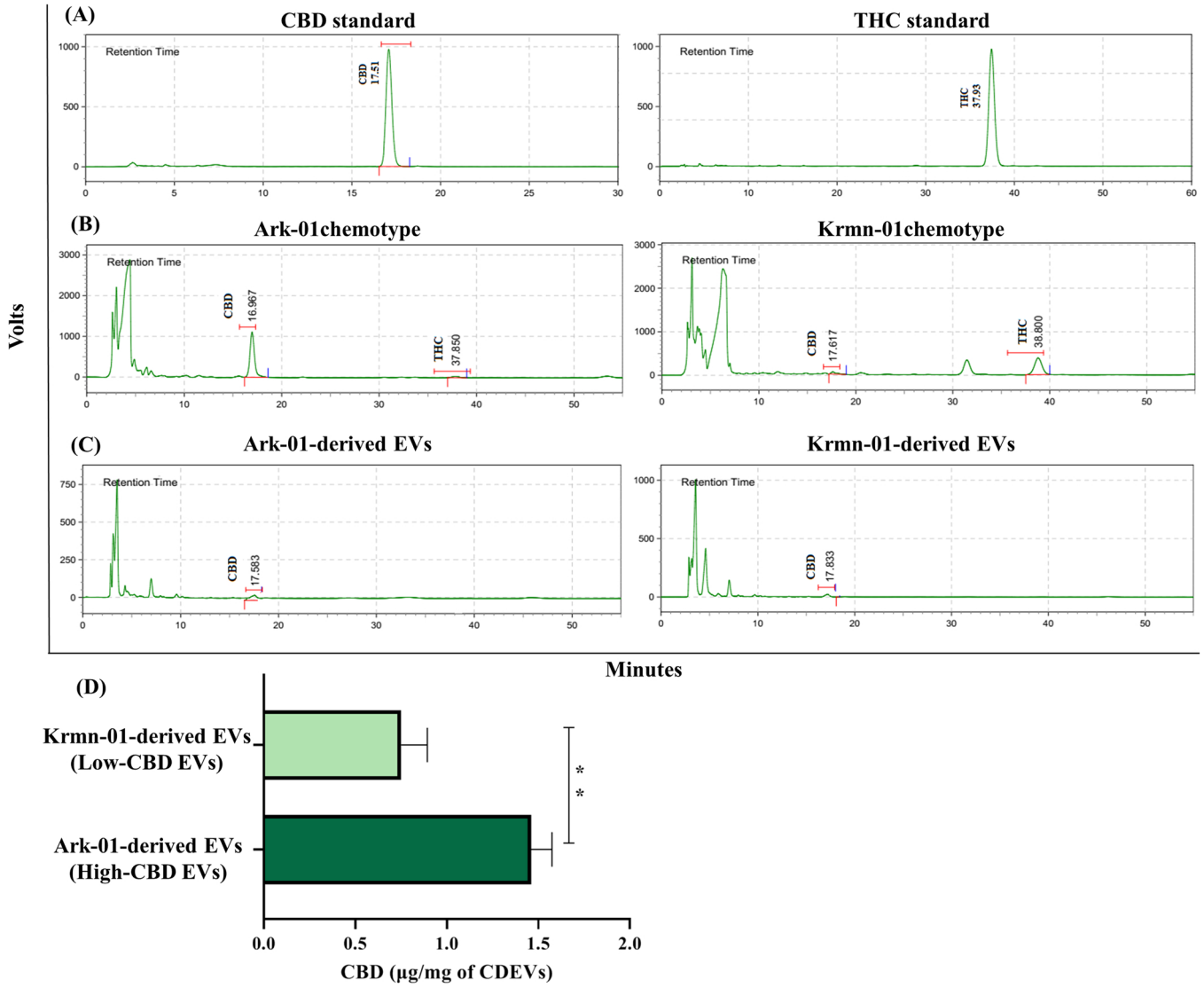


**Fig. 3.** Evaluation of the contents of THC and CBD in Ark-01 and Krmn-01 chemotypes and their corresponding EVs, Ark-01-derived EVs, and Krmn-01-derived EVs using HPLC. (A) The presence of THC and CBD were confirmed by valid standards and quantified using a calibration curve for each individual component (n = 3). (B) HPLC chromatograms of THC and CBD in cannabis extracts of Ark-01 and Krmn-01 chemotypes. (C) HPLC chromatograms of THC and CBD in CDEVs of Ark-01- and Krmn-01-derived EVs. (D) Quantification of CBD in extracts from Ark-01- and Krmn-01-derived EVs. The results were shown as the means ± SD of three independent experiments. The significant difference between two groups was calculated using unpaired Student's t-test (**$p < 0.01$).

B). Conversely, L.C-EVs treatment showed no significant effect on apoptosis of Huh-7 and HepG2 cells in 100 µg/ml, but relatively increased rate of apoptosis in the concentration of 150 µg/ml compared to the control cells ($p < 0.05$).

The apoptosis percentage of HepG2 cells significantly increased from 4.68 ± 2.33 % in the untreated cells to 16.81 ± 4.71 % ($p < 0.05$) following treatment with 150 µg/ml L.C-EVs (Fig. 5A and B). Similarly, the rate of apoptosis in Huh-7 cells relatively increased from 6.52 ± 3.32 % in the control cells to 15.21 ± 5.04 % ($p < 0.05$) in the concentrations of 150 µg/ml L.C-EVs (Fig. 6A and B). Given that the concentration of 100 µg/ml of L.C-EVs was not significant in the induction of apoptosis in both HCC cell lines, the dose of 150 µg/ml was chosen for conducting the following experiment.

### 3.5. CDEVs-induced HCC cell cycle arrest

With the intention of further investigating the inhibitory effect of CDEVs on HepG2 and Huh-7 cells proliferation, the cell cycle distribution in different phases was examined following treatment with 150 µg/ml of H.C-EVs and L.C-EVs. Flow cytometry results showed that H.C-EVs significantly caused a G0/G1 phase arrest in HepG2 and Huh-7 cells compared to the control group ($p < 0.01$). About 70 % of HepG2 cells and 64 % of Huh-7 cells accumulated in the G0/G1 phase after treatment with H.C-EVs. Concomitantly, a significant decrease in the number of cells in the S phase was also observed ($p < 0.05$). On the other hand, L.C-EVs induced the G0/G1 phase arrest in HepG2 cells, however significantly less than H.C-EVs ($p < 0.05$). Whereas, no significant difference was found in the proportion of Huh-7 cells at the G0–G1 phase, between L.C-EVs treatment and the control cells (Fig. 7).

### 3.6. Mitochondrial apoptosis pathway induction by H.C-EVs

From the apoptosis assay conducted, it was found that the mode of cell death induced by EVs isolated from the cannabis has to be via apoptosis. Considering the more statistically significant effects of H.C-EVs in the mentioned cellular assays, molecular investigations were performed after treatment with H.C-EVs. The effectiveness of H.C-EVs in modulating the expression of some important apoptotic genes (*BAX*, *Bcl-*

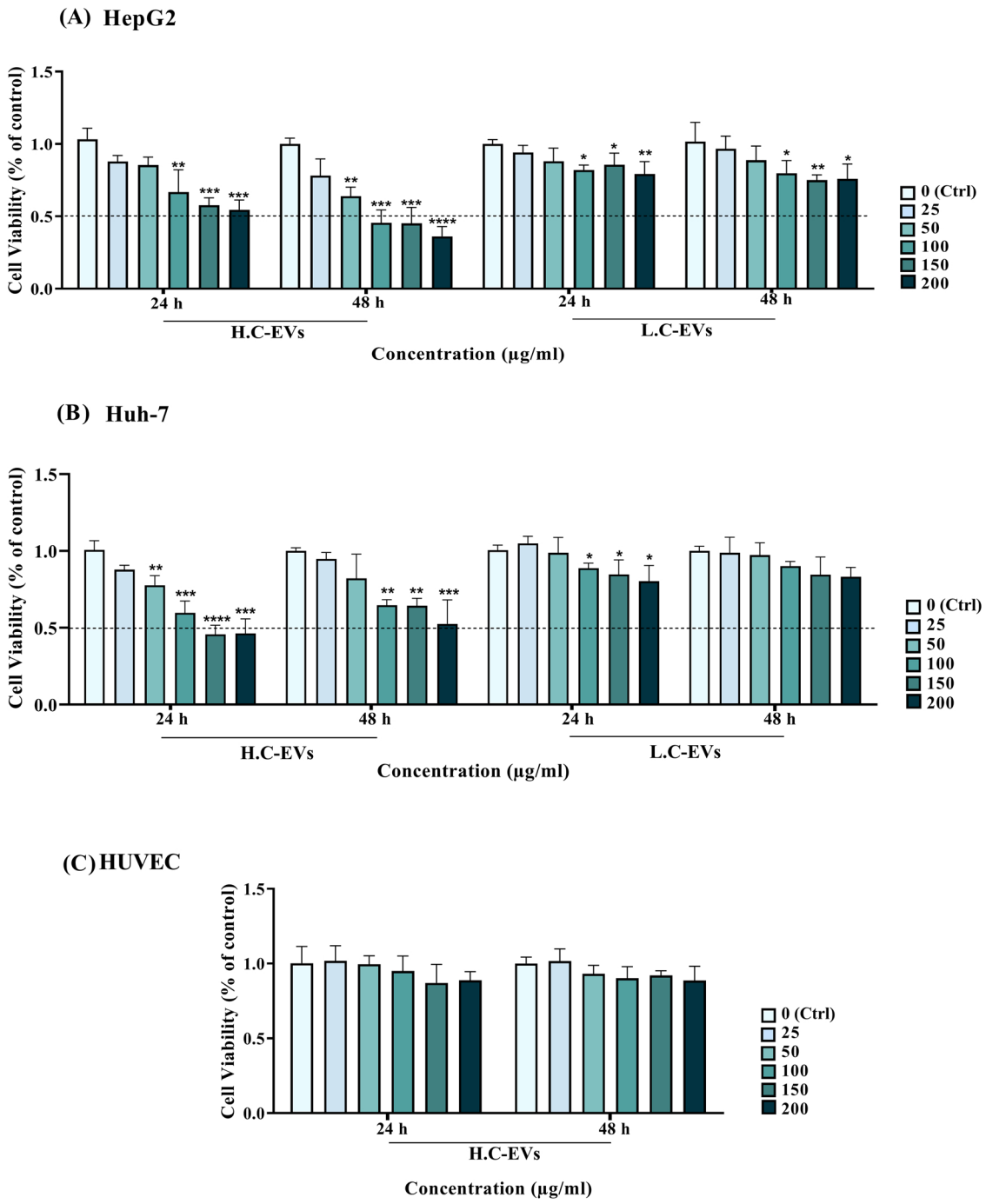


**Fig. 4.** Evaluation of the cytotoxic effect of CDEVs on two liver cancer cell lines and one normal cell line by MTT assay. (A) The cell viability percentage of HepG2 and (B) Huh-7 following treatment with five different concentrations of H.C-EVs and L.C-EVs for 24 and 48 h. The H.C-EVs severely inhibited the viability of Huh-7 and HepG2 cells after 24 h and 48 h, respectively. The L.C-EVs gradually reduced the viability of both cell lines. (C) Viability percentage of HUVECs cells following treatment with H.C-EVs for 24 and 48 h. The H.C-EVs didn't show significant cytotoxicity in HUVECs cells. The results were shown as the means ± SD of three independent experiments. The significant difference with the control was carried out at *$p < 0.05$, **$p < 0.01$, ***$p < 0.001$ and ****$p < 0.0001$.

*xl*, *CASP3*, *CASP8*, and *CASP9*) was evaluated in HepG2 and Huh-7 cell lines by qRT-PCR (Fig. 8). The qRT-PCR analysis revealed that H.C-EVs remarkably caused an upregulation in the pro-apoptotic marker, *BAX*, while simultaneously down-regulated the anti-apoptotic marker, *Bcl-xl* (a member of the Bcl-2 family) in the two HCC lines. Accordingly, following treatment with H.C-EVs, the expression level of *BAX* was significantly increased in HepG2 and Huh-7 cells compared to untreated control groups, ($p < 0.001$; relative expression: 3.41 ± 0.13 vs 1.07 ± 0.09 and 2.98 ± 0.33 vs 1.04 ± 0.02, respectively). Also, the relative expression of *Bcl-xl* was markedly decreased from 1.03 ± 0.06 (untreated HepG2) to 0.71 ± 0.12 (treated HepG2) and from 1.02 ± 0.04 (untreated Huh-7) to 0.55 ± 0.08 (treated in Huh-7).

Given that the mitochondria-mediated caspase-dependent pathway is a major apoptotic pathway, the expression levels of *CASP3*, *CASP9*, and *CASP8* genes were examined. Compared to the untreated control cells, H.C-EVs-treated HepG2 and Huh-7 cells demonstrated a significant rise in the expression levels of *CASP3* and *CASP9* transcripts (Fig. 8). The relative expression of *CASP3* increased in HepG2 and Huh-7 cells, respectively from 1.05 ± 0.08 and 1.03 ± 0.05 in the untreated cells to 2.55 ± 0.26 and 2.95 ± 0.31 in the cells co-cultured with H.C-EVs.

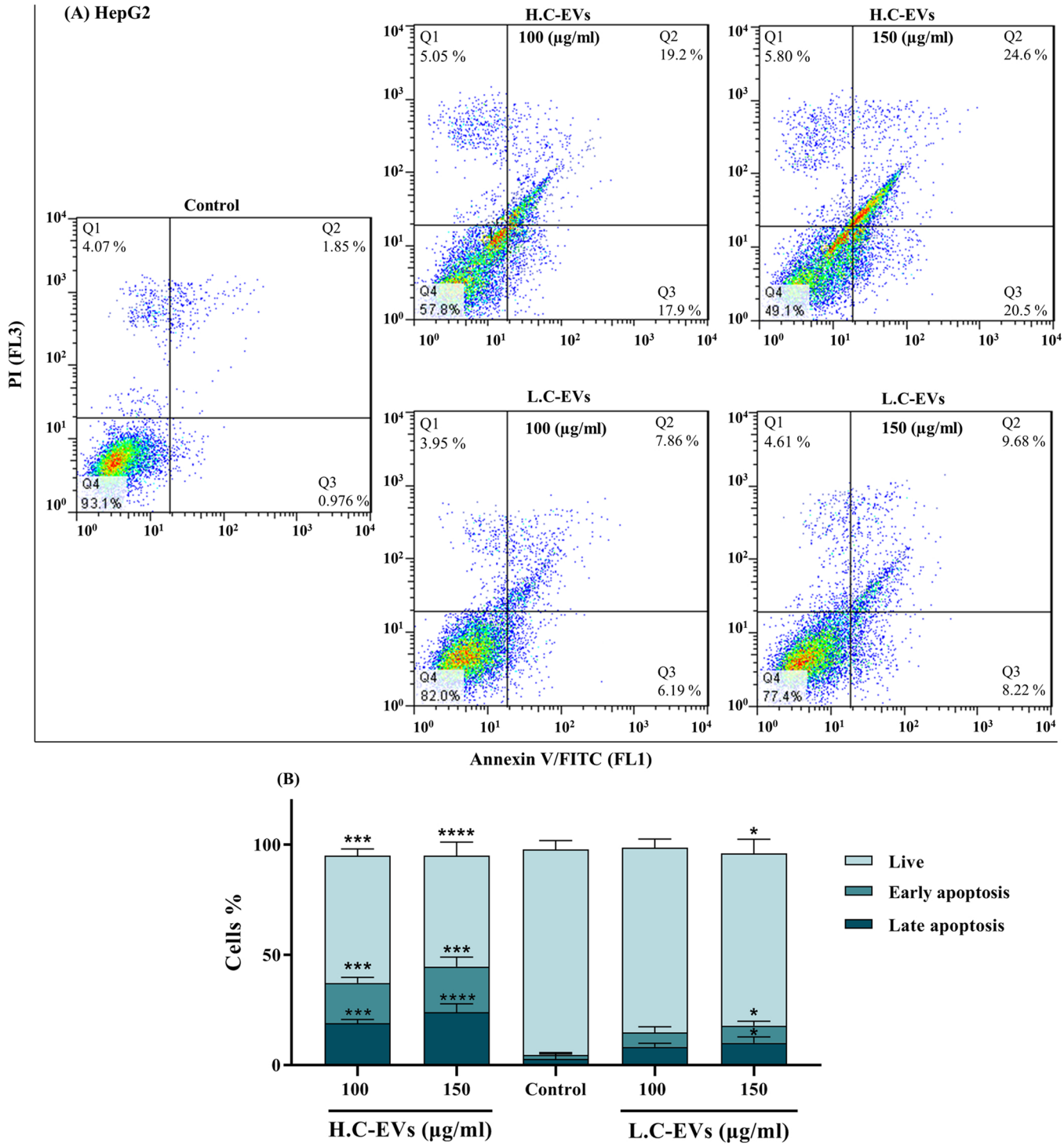


**Fig. 5.** The effect of CDEVs on apoptosis of HepG2 cells. (A) The cells were treated with 100 and 150 µg/ml of H.C-EVs and L.C-EVs for 48 h and apoptosis percentage was determined by Annexin V-FITC/PI double staining assay. Following treatment with H.C-EVs, the apoptosis rate (Q2 + Q3) of HepG2 cells significantly increased in a dose-dependent manner. The L.C-EVs could not significantly induce apoptosis in the concentration of 100 µg/ml, but induced at 150 µg/ml. (B) Statistical analysis of the apoptosis percentage of the HepG2 cells. All data are presented as the mean ± SD of three independent experiments. The significant difference with the control was carried out at $^{*}p < 0.05$, $^{**}p < 0.01$, $^{***}p < 0.001$ and $^{****}p < 0.0001$.

Moreover, similar results were observed in the relative expression of *CASP9* that significantly up-regulated in both HCC cells treated with H. C-EVs in comparison with the untreated control cells ($p < 0.01$). The H. C-EVs treatment caused a significant increase in the expression level of *CASP8* from 1.01 ± 0.04–1.32 ± 0.17 in HepG2 cells ($p < 0.01$) and from 1.03 ± 0.05–1.23 ± 0.11 in Huh-7 cells ($p < 0.05$), compared to the control cells.

## 4. Discussion

For thousands of years, extracts and other derivatives of plants have been widely used in traditional medicine, due to the content of their therapeutic phytochemicals [53]. Recently, researchers have proven that plant extracts [54], fruits juice [55,56], herbal decoction [57], and plants sap [30] contain stable and bioactive EVs [54]. Increasing

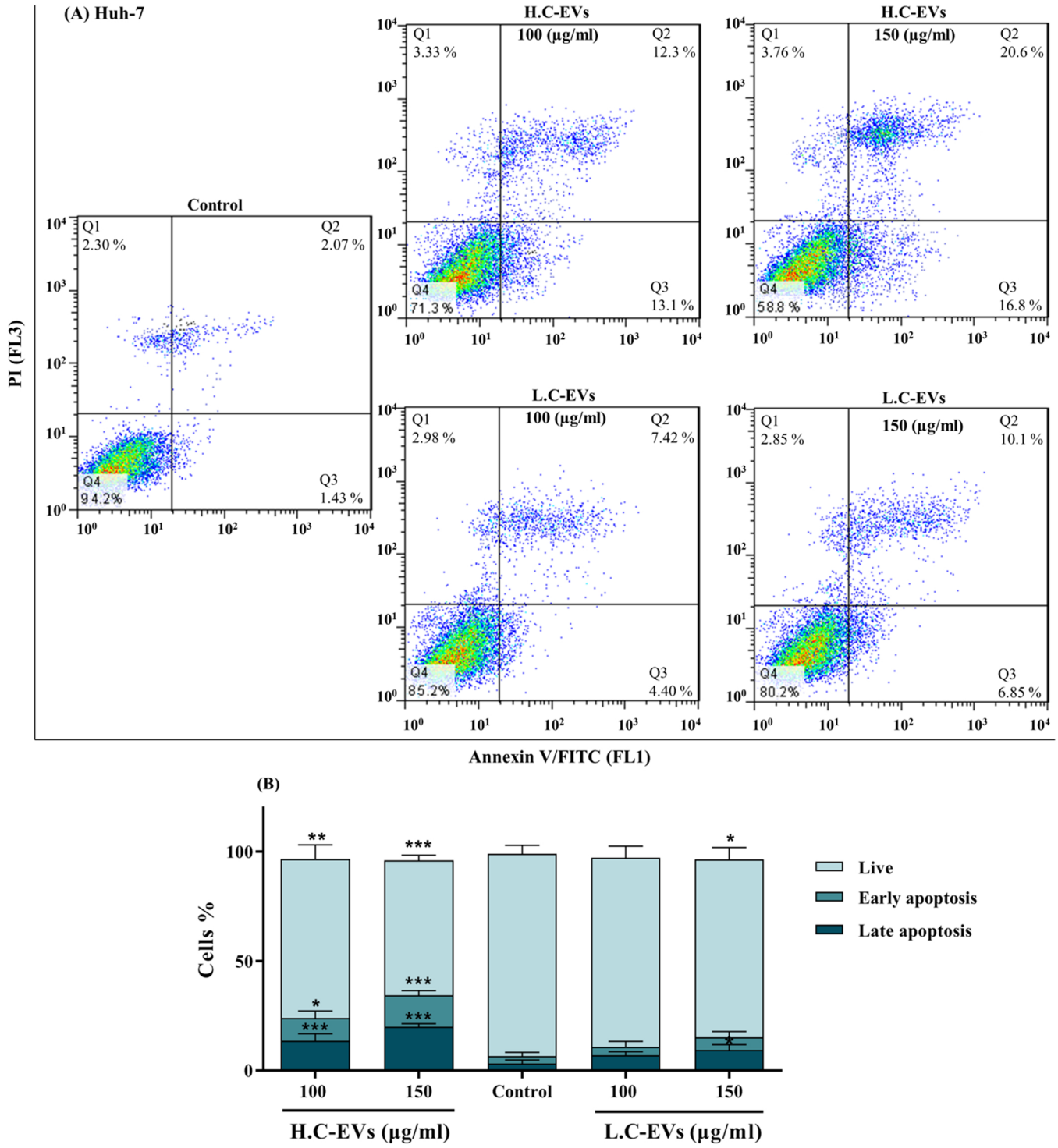


**Fig. 6.** The effect of CDEVs on apoptosis of Huh-7 cells. (A) The cells were treated with 100 and 150 µg/ml of H.C-EVs and L.C-EVs for 24 h and apoptosis rate was determined by Annexin V-FITC/PI double staining and a flow cytometer instrument. Following treatment with H.C-EVs, the apoptosis percentage (Q2 + Q3) of cells significantly increased in a dose-dependent manner whereas L.C-EVs could not effectively induce apoptosis in concentration of 100 µg/ml. (B) Statistical analysis of the apoptosis percentage of the Huh-7 cells. All data are presented as the mean ± SD of three independent experiments. The significant difference with the control was carried out at $*p < 0.05$, $**p < 0.01$, *** and $p < 0.001$.

evidence suggests that plant-derived EVs have a high rate of internalization in specific mammalian cells such as intestinal stem cells [58], macrophages [23], or cancer cells [30]. They are involved in plant-animal cross-kingdom communication, transfer their endogenous bioactive molecules to recipient cells, and trigger cellular and molecular responses [24,59]. Thus, plant-derived EVs can be used in therapeutic fields [60].

Here, it was hypothesized that cannabis plant extract contains EVs that may deliver their intrinsic therapeutics phytochemicals to cancer cells and show anticancer effects. Numerous data suggest the potential functionality of cannabis phytocannabinoids, especially CBD and THC, in cancer treatment [61,62]. Due to THC psychoactive effects, using this

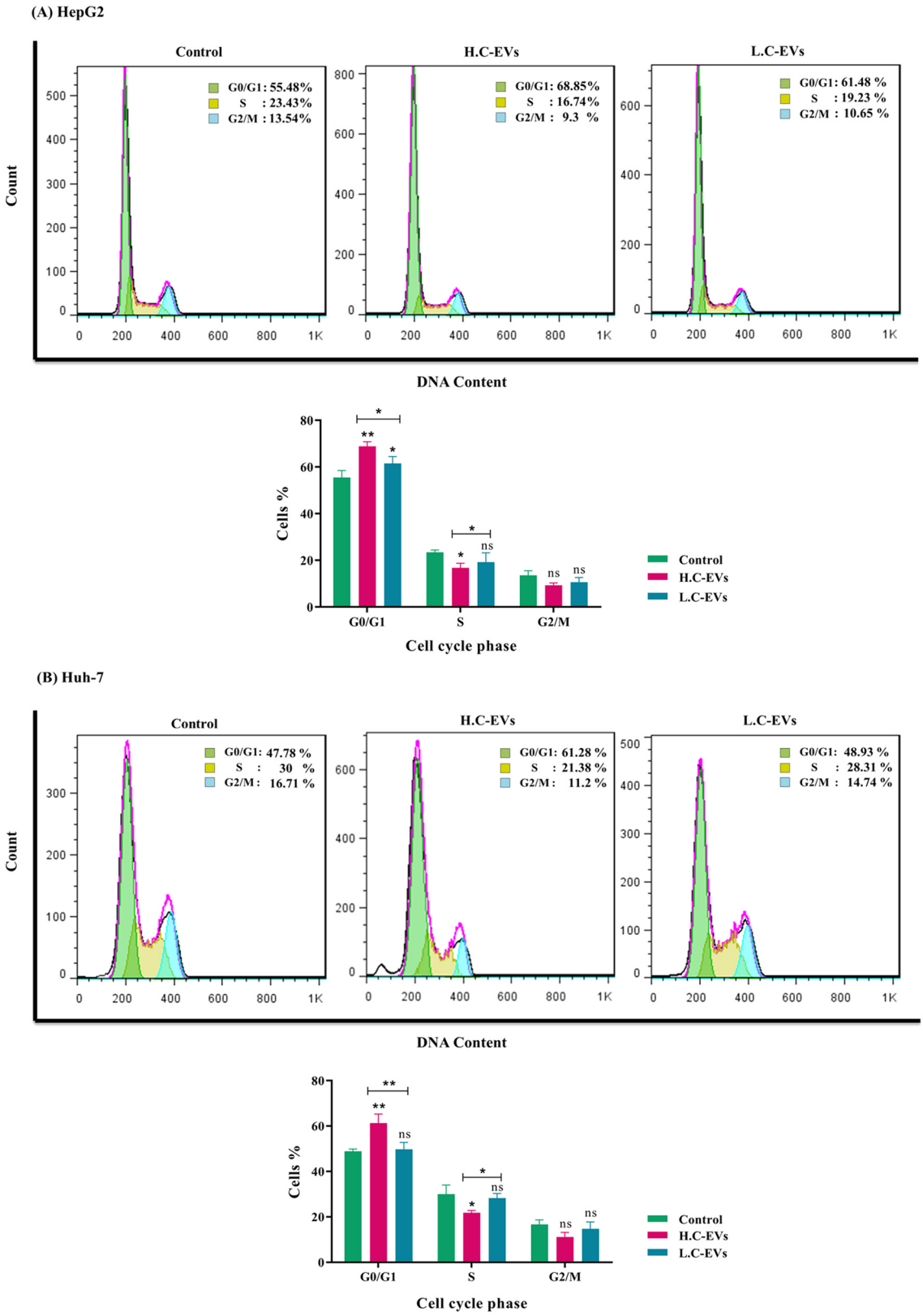


**Fig. 7.** Effect of CDEVs on cell cycle distribution of HCC cells. (A) Cell cycle analysis of HepG2 by flow cytometry, after exposure to 150 μg/ml H.C-EVs and L.C-EVs for 48 h. (B) Flow cytometry analysis of cell cycle phases of Huh-7, after exposure to 150 μg/ml H.C-EVs and L.C-EVs for 24 h. The H.C-EVs treatment significantly increased the proportion of the G1/G0 phase in HepG2 and Huh-7 cells compared to the control groups, while significantly decreased the S phase. The L.C-EVs treatment also showed a significant effect on G0/G1 phase arrest in HepG2, however was less than H.C-EVs. In contrast, L.C-EVs didn't significantly affect the Huh-7 cell cycle distribution. Data are expressed as the mean ± SD (n = 3). The significant difference with the control and between two groups were carried out at $*p < 0.05$ and $**p < 0.01$. ns: non-significant.

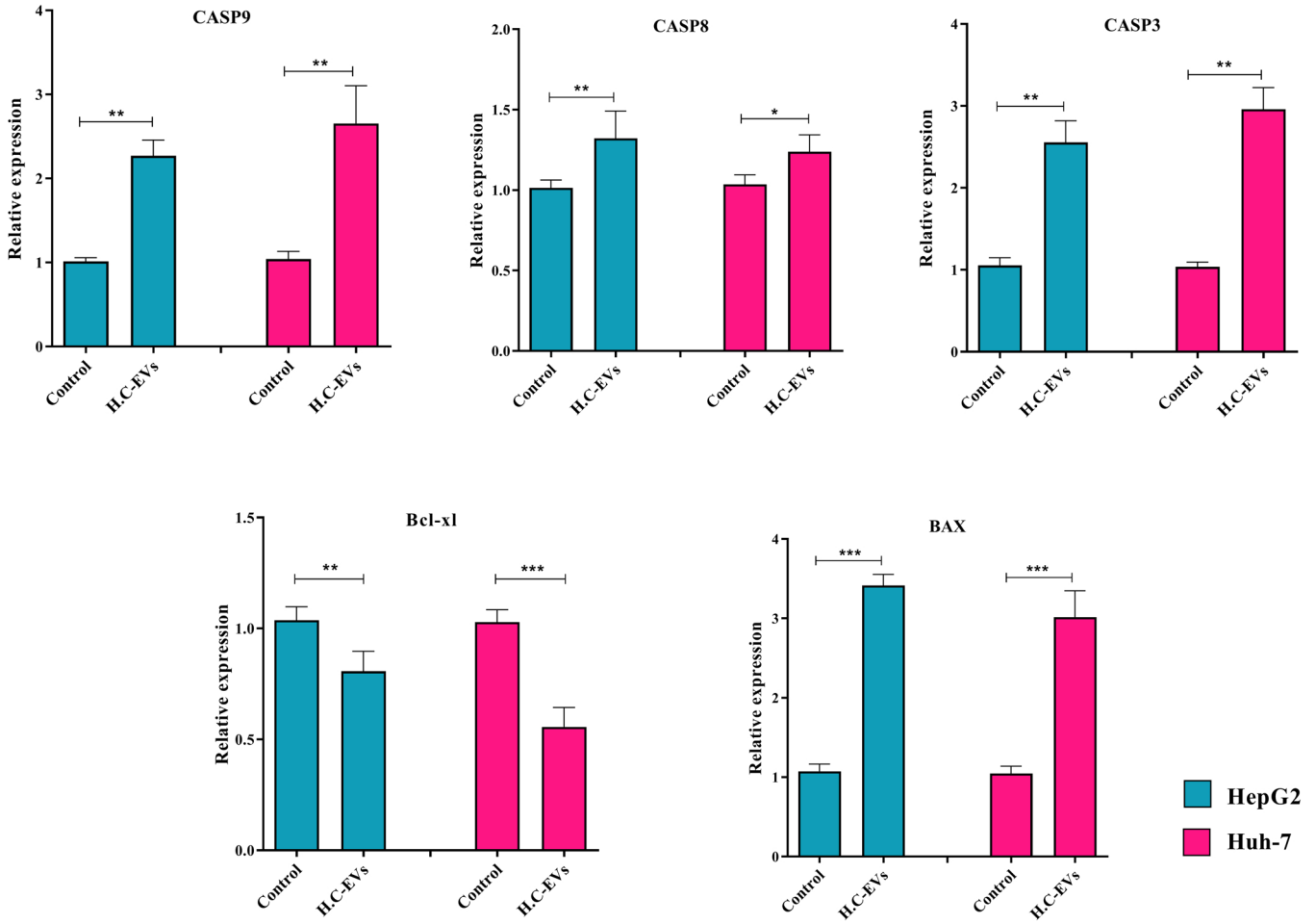


**Fig. 8.** H.C-EVs induced mitochondrial-mediated apoptosis in HepG2 and Huh-7 cells. Relative expression levels of *CASP3*, *CASP8*, *CASP9*, *BAX*, and *Bcl-xl* by qRT-PCR, following the treatment with a moderate concentration (100 μg/ml) of H.C-EVs, in HepG2 and Huh-7 cell lines, respectively. Amplification of PCR was normalized against *GAPDH*. The values are shown as mean ± SD of three independent experiments. The significant difference with the control (untreated cells) was carried out at $*p < 0.05$, $**p < 0.01$, and $***p < 0.001$.

compound or D9-THC-related cannabinoids is limited in cancer research [63]. In contrast, CBD has recently received a lot of attention in many therapeutic studies on cancer [64].

In the current study, EVs were isolated from two cannabis chemotypes and characterized. The differential ultra-centrifugation plus sucrose density gradient method was selected for the isolation of EVs as reported for several other plant species such as grape, carrot [22], grapefruit [23], ginger [7], tomato [11], and clementine fruit [65]. Isolated EVs from two cannabis chemotypes had a single peak in size distribution graphs with a size range of ~30–250 nm. Previously, the broad size distribution of plant-EVs between 30 and 500 nm was reported [12]. Isolated CDEVs were monodisperse, differing in average size with the EVs derived from other plants which suggest the plant's EVs size is species-specific [22,66].

The presence of secondary metabolites encapsulated within plant-EVs can enhance their biological effects [21]. Therefore, it is necessary to know the phytochemicals and inner secondary metabolites of plant EVs, to improve our understanding of their biological effects [67]. Here, two chemotypes with different CBD and THC contents were chosen and HPLC separation of CDEVs was illustrative of the absence of THC, but different contents of CBD were evident as H.C-EVs (high CBD content) and L.C-EVs (low CBD content). Similarly, the presence of major metabolites such as naringin, naringenin [23], shogaol [24], and sulforaphane [68] were detected in EVs extracted from grapefruit, ginger, and broccoli, respectively. Whereas, the absence of vitamin C and naringenin (two major active compounds in orange juice) was reported in orange nanovesicles [69]. In addition, Stanly and colleagues revealed that the metabolic profile of grapefruit-derived nanovesicles was different from grapefruit juice [67].

Generally, earlier studies in line with our findings suggest that the presence of a phytochemical in the plant of origin does not necessarily mean its presence within the EVs. Based on HPLC observations, it was postulated that H.C-EVs and L.C-EVs have their own specific bioactive properties.

To determine whether H.C-EVs and L.C-EVs have different biological effects on the viability of cancer cells, their cytotoxicity effects were investigated on two HCC cell lines; HepG2 and Huh-7. H.C-EVs strongly decreased the viability of HepG2 and Huh-7 cancer cells in a dose and time-dependent manner compared with L.C-EVs. In fact, H.C-EVs showed higher cytotoxicity than L.C-EVs, probably due to their different metabolic content, including CBD. The selectively concentration-dependent killing effects of CBD have been demonstrated in some cancer cell lines, including HepG2 [42,70,71]. Although H.C-EVs considerably reduced HCC cells viability, they had no significant effect on HUVECs normal cells growth. These results probably suggested a specific effect of H.C-EVs on cancer cells. In line with our results, Kim and colleagues showed that EVs isolated from *Dendropanax morbifera* and *Pinus densiflora* saps exerted remarkable cytotoxic effects on breast and skin cancer cells without substantial effect on normal cells [30]. In that report, they inferred that normal and tumor breast cells use different endocytosis pathways to internalize the plant sap-derived EVs. The caveolae-mediated endocytosis was confirmed as the predominant

internalization pathway in MDA-MB-231 and MCF7 cancer cells that prevents degradation of EVs by the lysosome. In contrast, the internalization of plant sap-derived EVs in breast normal cells occurred mainly via micropinocytosis, that it leads to EVs degradation by lysosomes degradative compartment [30]. In another study, micro- and nano-vesicles purified from four citrus species inhibited the proliferation of lung, skin, and breast cancer cell lines without a negative effect on the growth of non-cancer cells (HaCaT, human keratinocytes). It was suggested that the content of citrus-derived vesicles is safe for normal cells but has specific bioactivity on cancer cells [67]. It seems some phytochemicals have a selective function on cancer cells, without a significant effect on normal cells [72].

The most common causes of cancer relate back to the defection in the cell cycle, the corresponding checkpoints, and the dysfunction of apoptotic machinery that show the main therapeutic targets for the treatment of cancer [73]. In the continuation of comparative functional analyses of the two CDEVs populations (H.C-EVs and L.C-EVs), H.C-EVs showed to impair the cell cycle of HepG2 and Huh7 more effectively. The H.C-EVs arrested G0/G1 phase and reduced the S phase in the cell cycle which shows they can affect the proliferation of two liver cancer cell lines. It has been reported that CBD exerts its function through distinct mechanisms acting on the cell cycle, autophagy, apoptosis, and metastasis [63]. The CBD blocked cell cycle progression in the G0/G1 phase and reduced cell proliferation in MCF-7 and MDA-MB-231 breast cancer cells [38], human leukemic Jurkat cells [74], LNCaP and PC3 prostate cancer cells [73], and SGC-7901 gastric cancer cells [75].

Apoptosis assay results revealed that H.C-EVs induced apoptosis in HepG2 and Huh7 cells in a dose-dependent manner, more effective than L.C-EVs. As a result, the pro-apoptotic effects of H.C-EVs on the apoptosis signaling pathway were analyzed. The H.C-EVs triggered apoptosis by the decrease in the mRNA levels of the *Bcl-2* gene and together with the increase in the mRNA levels of *BAX*, *CASP3*, *CASP8*, and *CASP9* genes in HepG2 and Huh-7 cell lines. The pro-apoptotic gene, *BAX*, and pro-survival gene, *Bcl-2* regulate apoptosis via the mitochondria and are principally involved in the regulation of the apoptosis intrinsic pathway [76]. The *Bcl-2* family, such as *Bcl-xl*, prevents apoptotic death [77]. Conversely, *BAX* is mainly involved in the induction of apoptosis through the initiator caspases activation [76]. The caspases are known as effector molecules in different types of cell death and are involved in the execution of apoptosis [78]. CASP9 and CASP8 act as effector proteins in the initiation of apoptosis. CASP3 has a key role in the caspases cascade to execute apoptosis. Increasing CASP8 and CASP9 within a cancer cell, promote the cleavage of CASP3 that leads to programmed cell death [79,80]. We demonstrated that H.C-EVs induced apoptosis through a mitochondrial-dependent apoptosis signaling pathway in two HCC cell lines, suggesting that H.C-EVs can be potentially used as a novel biomaterial in inhibiting cancer cells.

Several studies reported that CBD-rich cannabis extract or purified CBD compound have anti-proliferative and anti-cancer effects on the variety of cancer cells both in vitro and in mouse tumor models without a remarkable effect on normal cells [39,70,75,81,82]. However, further research is needed to exactly determine which inner bioactive compound from H.C-EVs play an effector role towards their anticancer effects.

## 5. Conclusion

EVs from two *Cannabis sativa* chemotypes with different ratios of CBD and THC were isolated and their potential antineoplastic properties were checked for the first time. Our findings revealed that EVs derived from the two chemotypes only contained CBD; lacking THC. Isolated CDEVs with higher CBD content decreased the viability of two liver cancer cell lines more effectively compared to CDEVs with lower CBD content; with no effect on HUVECs' normal cells. In addition, the mechanism by which H.C-EVs exerted the in vitro anticancer activity involved cell cycle arrest in the G0/G1 phase as well as induction of apoptosis via mitochondrial-dependent apoptosis signaling pathway. Altogether, our findings suggest that the EVs derived from cannabis can act as natural nano-carriers containing bioactive phytochemicals and be used in cancer research. The possible use of these biomaterials in combination with chemotherapy drugs can open a new gateway for cancer treatment.

## CRediT authorship contribution statement

**Tahereh Tajik:** Investigation, Methodology, Execution, Analysis, Visualization, Writing – original draft. **Kaveh Baghaei:** Methodology and study design, Project administration, Writing – review & editing. **Vahid Erfani Moghadam:** Methodology, Supervision. **Naser Farrokhi:** Supervision, Writing – review & editing. **Seyed Alireza Salami:** Preparation of plant material, HPLC analysis.

## Funding

This research received no external funding.

## Conflict of interest statement

The authors declare no conflict of interest.

## Data Availability

No data was used for the research described in the article.

## Acknowledgments

Authors would like to acknowledge both Shahid Beheshti University and the Research Institute for Gastroenterology and Liver Diseases (RIGLD) at Shahid Beheshti University of Medical Sciences (Tehran, Iran) for supporting this study. Also, the authors appreciate the Center for Genetic Resources of Cannabis, Iran (CGRC, www.medcanabase.org) for donating two cannabis chemotypes.

## References

[1] J.R. Sotelo, K.R. Porter, An electron microscope study of the rat ovum, J. Biophys. Biochem. Cytol. 5 (1959) 327–342, https://doi.org/10.1083/jcb.5.2.327.
[2] E. Woith, G. Fuhrmann, M.F. Melzig, Extracellular vesicles—connecting kingdoms, Int. J. Mol. Sci. 20 (2019) 5695, https://doi.org/10.3390/ijms20225695.
[3] L.M. Doyle, M.Z. Wang, Overview of extracellular vesicles, their origin, composition, purpose, and methods for exosome isolation and analysis, Cells 8 (2019) 727, https://doi.org/10.3390/cells8070727.
[4] M. Yáñez-Mó, P.R.-M. Siljander, Z. Andreu, A. Bedina Zavec, F.E. Borràs, E.I. Buzas, K. Buzas, E. Casal, F. Cappello, J. Carvalho, Biological properties of extracellular vesicles and their physiological functions, J. Extra Vesicles 4 (2015) 27066, https://doi.org/10.3402/jev.v4.27066.
[5] D. Sun, X. Zhuang, X. Xiang, Y. Liu, S. Zhang, C. Liu, S. Barnes, W. Grizzle, D. Miller, H.-G. Zhang, A novel nanoparticle drug delivery system: the anti-inflammatory activity of curcumin is enhanced when encapsulated in exosomes, Mol. Ther. 18 (2010) 1606–1614, https://doi.org/10.1038/mt.2010.105.
[6] S. Raimondo, G. Giavaresi, A. Lorico, R. Alessandro, Extracellular vesicles as biological shuttles for targeted therapies, Int. J. Mol. Sci. 20 (2019) 1848, https://doi.org/10.3390/ijms20081848.
[7] M. Zhang, B. Xiao, H. Wang, M.K. Han, Z. Zhang, E. Viennois, C. Xu, D. Merlin, Edible ginger-derived nano-lipids loaded with doxorubicin as a novel drug-delivery approach for colon cancer therapy, Mol. Ther. 24 (2016) 1783–1796, https://doi.org/10.1038/mt.2016.159.
[8] S. Fais, L. O'Driscoll, F.E. Borras, E. Buzas, G. Camussi, F. Cappello, J. Carvalho, A. C. Da Silva, H. Del Portillo, S. El Andaloussi, Evidence-based clinical use of nanoscale extracellular vesicles in nanomedicine, ACS Nano 10 (2016) 3886–3899, https://doi.org/10.1021/acsnano.5b08015.
[9] M. Malloci, L. Perdomo, M. Veerasamy, R. Andriantsitohaina, G. Simard, M. C. Martínez, Extracellular vesicles: mechanisms in human health and disease, Antioxid. Redox Signal. 30 (2019) 813–856, https://doi.org/10.1089/ars.2017.7265.
[10] F. Properzi, M. Logozzi, S. Fais, Exosomes: the future of biomarkers in medicine, Biomark. Med. 7 (2013) 769–778, https://doi.org/10.2217/bmm.13.63.
[11] R. Bokka, A.P. Ramos, I. Fiume, M. Manno, S. Raccosta, L. Turiák, S. Sugár, G. Adamo, T. Csizmadia, G. Pocsfalvi, Biomanufacturing of tomato-derived nanovesicles, Foods 9 (2020) 1852, https://doi.org/10.3390/foods9121852.

[12] C. Yang, M. Zhang, D. Merlin, Advances in plant-derived edible nanoparticle-based lipid nano-drug delivery systems as therapeutic nanomedicines, J. Mater. Chem. B 6 (2018) 1312–1321, https://doi.org/10.1039/C7TB03207B.
[13] W. Halperin, W.A. Jensen, Ultrastructural changes during growth and embryogenesis in carrot cell cultures, J. Ultra Res. 18 (1967) 428–443, https://doi.org/10.1016/s0022-5320(67)80128-x.
[14] R. Marchant, A. Robards, Membrane systems associated with the plasmalemma of plant cells, Ann. Bot. 32 (1968) 457–471, https://doi.org/10.1093/OXFORDJOURNALS.AOB.A084221.
[15] M. Regente, M. Pinedo, M. Elizalde, L. de la Canal, Apoplastic exosome-like vesicles: a new way of protein secretion in plants? Plant Signal Behav. 7 (2012) 544–546, https://doi.org/10.4161/psb.19675.
[16] Q. An, A.J. van Bel, R. Hückelhoven, Do plant cells secrete exosomes derived from multivesicular bodies? Plant Signal Behav. 2 (2007) 4–7, https://doi.org/10.4161/psb.2.1.3596.
[17] L.L. Hansen, M.E. Nielsen, Plant exosomes: using an unconventional exit to prevent pathogen entry? J. Exp. Bot. 69 (2018) 59–68, https://doi.org/10.1093/jxb/erx319.
[18] K. Miyado, W. Kang, K. Yamatoya, M. Hanai, A. Nakamura, T. Mori, M. Miyado, N. Kawano, Exosomes versus microexosomes: shared components but distinct functions, J. Plant Res. 130 (2017) 479–483, https://doi.org/10.1007/s10265-017-0907-7.
[19] M. Zhang, E. Viennois, C. Xu, D. Merlin, Plant derived edible nanoparticles as a new therapeutic approach against diseases, Tissue Barriers 4 (2016), e1134415, https://doi.org/10.1080/21688370.2015.1134415.
[20] P. Akuma, O.D. Okagu, C.C. Udenigwe, Naturally occurring exosome vesicles as potential delivery vehicle for bioactive compounds, Front. Sustain. Food Syst. 3 (2019) 23, https://doi.org/10.3389/fsufs.2019.00023.
[21] E. Woith, G. Guerriero, J.-F. Hausman, J. Renaut, C.C. Leclercq, C. Weise, S. Legay, A. Weng, M.F. Melzig, Plant extracellular vesicles and nanovesicles: focus on secondary metabolites, proteins and lipids with perspectives on their potential and sources, Int. J. Mol. Sci. 22 (2021) 3719, https://doi.org/10.3390/ijms22073719.
[22] J. Mu, X. Zhuang, Q. Wang, H. Jiang, Z. Deng, B. Wang, L. Zhang, S. Kakar, Y. Jun, D. Miller, Interspecies communication between plant and mouse gut host cells through edible plant derived exosome-like nanoparticles, Mol. Nutr. Food Res. 58 (2014) 1561–1573, https://doi.org/10.1002/mnfr.201300729.
[23] B. Wang, X. Zhuang, Z.-B. Deng, H. Jiang, J. Mu, Q. Wang, X. Xiang, H. Guo, L. Zhang, G. Dryden, Targeted drug delivery to intestinal macrophages by bioactive nanovesicles released from grapefruit, Mol. Ther. 22 (2014) 522–534, https://doi.org/10.1038/mt.2013.190.
[24] X. Zhuang, Z.-B. Deng, J. Mu, L. Zhang, J. Yan, D. Miller, W. Feng, C.J. McClain, H.-G. Zhang, Ginger-derived nanoparticles protect against alcohol-induced liver damage, J. Extra Vesicles 4 (2015) 28713, https://doi.org/10.3402/jev.v4.28713.
[25] Z. Li, H. Wang, H. Yin, C. Bennett, H. Zhang, P. Guo, Arrowtail RNA for ligand display on ginger exosome-like nanovesicles to systemic deliver siRNA for cancer suppression, Sci. Rep. 8 (2018) 1–11, https://doi.org/10.1038/s41598-018-32953-7.
[26] M. Zhang, E. Viennois, M. Prasad, Y. Zhang, L. Wang, Z. Zhang, M.K. Han, B. Xiao, C. Xu, S. Srinivasan, Edible ginger-derived nanoparticles: A novel therapeutic approach for the prevention and treatment of inflammatory bowel disease and colitis-associated cancer, Biomaterials 101 (2016) 321–340, https://doi.org/10.1016/j.biomaterials.2016.06.018.
[27] R. Lee, H.J. Ko, K. Kim, Y. Sohn, S.Y. Min, J.A. Kim, D. Na, J.H. Yeon, Anti-melanogenic effects of extracellular vesicles derived from plant leaves and stems in mouse melanoma cells and human healthy skin, J. Extra Vesicles 9 (2020) 1703480, https://doi.org/10.1080/20013078.2019.1703480.
[28] S. Raimondo, F. Naselli, S. Fontana, F. Monteleone, A.L. Dico, L. Saieva, G. Zito, A. Flugy, M. Manno, M.A.Di Bella, Citrus limon-derived nanovesicles inhibit cancer cell proliferation and suppress CML xenograft growth by inducing TRAIL-mediated cell death, Oncotarget 6 (2015) 19514, https://doi.org/10.18632/oncotarget.4004.
[29] M. Yang, X. Liu, Q. Luo, L. Xu, F. Chen, An efficient method to isolate lemon derived extracellular vesicles for gastric cancer therapy, J. Nanobiotechnol. 18 (2020) 1–12, https://doi.org/10.1186/s12951-020-00656-9.
[30] K. Kim, H.J. Yoo, J.-H. Jung, R. Lee, J.-K. Hyun, J.-H. Park, D. Na, J.H. Yeon, Cytotoxic effects of plant sap-derived extracellular vesicles on various tumor cell types, J. Funct. Biomater. 11 (2020) 22, https://doi.org/10.3390/jfb11020022.
[31] S.A. Salami, F. Martinelli, A. Giovino, A. Bachari, N. Arad, N. Mantri, It is our turn to get cannabis high: put cannabinoids in food and health baskets, Molecules 25 (2020) 4036, https://doi.org/10.3390/molecules25184036.
[32] C.M. Andre, J.-F. Hausman, G. Guerriero, *Cannabis sativa*: the plant of the thousand and one molecules, Front. Plant Sci. 7 (2016) 19, https://doi.org/10.3389/fpls.2016.00019.
[33] P. Morales, N. Jagerovic, Antitumor cannabinoid chemotypes: structural insights, Front. Pharmacol. 10 (2019) 621, https://doi.org/10.3389/fphar.2019.00621.
[34] D.L. de Almeida, L.A. Devi, Diversity of molecular targets and signaling pathways for CBD, Pharmacol. Res. Perspect. 8 (2020), e00682, https://doi.org/10.1002/prp2.682.
[35] R.D. Richins, L. Rodriguez-Uribe, K. Lowe, R. Ferral, M.A. O'Connell, Accumulation of bioactive metabolites in cultivated medical Cannabis, PLoS One 13 (2018), e0201119, https://doi.org/10.1371/journal.pone.0201119.
[36] F. Afrin, M. Chi, A.L. Eamens, R.J. Duchatel, A.M. Douglas, J. Schneider, C. Gedye, A.S. Woldu, M.D. Dun, Can hemp help? Low-THC cannabis and non-THC cannabinoids for the treatment of cancer, Cancers 12 (2020) 1033, https://doi.org/10.3390/cancers12041033.
[37] S. Sreevalsan, S. Joseph, I. Jutooru, G. Chadalapaka, S.H. Safe, Induction of apoptosis by cannabinoids in prostate and colon cancer cells is phosphatase dependent, Anticancer Res. 31 (2011) 3799–3807.
[38] A. Ligresti, A.S. Moriello, K. Starowicz, I. Matias, S. Pisanti, L. De Petrocellis, C. Laezza, G. Portella, M. Bifulco, V. Di Marzo, Antitumor activity of plant cannabinoids with emphasis on the effect of cannabidiol on human breast carcinoma, J. Pharmacol. Exp. Ther. 318 (2006) 1375–1387, https://doi.org/10.1124/jpet.106.105247.
[39] S.T. Lukhele, L.R. Motadi, Cannabidiol rather than *Cannabis sativa* extracts inhibit cell growth and induce apoptosis in cervical cancer cells, BMC Complement. Med. Ther. 16 (2016) 1–16, https://doi.org/10.1186/s12906-016-1280-0.
[40] V. Bogdanović, J. Mrdjanović, I. Borišev, A review of the therapeutic antitumor potential of cannabinoids, J. Alter. Complement. Med. 23 (2017) 831–836, https://doi.org/10.1089/acm.2017.0016.
[41] R. Ramer, B. Hinz, Cannabinoids as anticancer drugs, Adv. Pharmacol. 80 (2017) 397–436, https://doi.org/10.1016/bs.apha.2017.04.002.
[42] U.S. Kosgodage, R. Mould, A.B. Henley, A.V. Nunn, G.W. Guy, E.L. Thomas, J. M. Inal, J.D. Bell, S. Lange, Cannabidiol (CBD) is a novel inhibitor for exosome and microvesicle (EMV) release in cancer, Front. Pharmacol. 9 (2018) 889, https://doi.org/10.3389/fphar.2018.00889.
[43] U.S. Kosgodage, P. Uysal-Onganer, A. MacLatchy, R. Mould, A.V. Nunn, G.W. Guy, I. Kraev, N.P. Chatterton, E.L. Thomas, J.M. Inal, Cannabidiol affects extracellular vesicle release, miR21 and miR126, and reduces prohibitin protein in glioblastoma multiforme cells, Transl. Oncol. 12 (2019) 513–522, https://doi.org/10.1016/j.tranon.2018.12.004.
[44] O.O. Ogunwobi, T. Harricharran, J. Huaman, A. Galuza, O. Odumuwagun, Y. Tan, G.X. Ma, M.T. Nguyen, Mechanisms of hepatocellular carcinoma progression, World J. Gastroenterol. 25 (2019) 2279, https://doi.org/10.3748/wjg.v25.i19.2279.
[45] H. Sung, J. Ferlay, R.L. Siegel, M. Laversanne, I. Soerjomataram, A. Jemal, F. Bray, Global cancer statistics 2020: GLOBOCAN estimates of incidence and mortality worldwide for 36 cancers in 185 countries, CA Cancer J. Clin. 71 (2021) 209–249, https://doi.org/10.3322/caac.21660.
[46] J. Ferlay, M. Ervik, F. Lam, M. Colombet, L. Mery, M. Piñeros, A. Znaor, I. Soerjomataram, F. Bray, Global Cancer Observatory: Cancer Today, IARC, 2018. https://gco.iarc.fr/today/home.
[47] D. Vara, M. Salazar, N. Olea-Herrero, M. Guzman, G. Velasco, I. Diaz-Laviada, Anti-tumoral action of cannabinoids on hepatocellular carcinoma: role of AMPK-dependent activation of autophagy, Cell Death Differ. 18 (2011) 1099–1111, https://doi.org/10.1038/cdd.2011.32.
[48] N.E. Ibrahim, W.M. Aboulthana, R.K. Sahu, Hepatocellular carcinoma: causes and prevention, UKJPB 6 (2018) 48–55, https://doi.org/10.20510/ukjpb/6/i5/177354.
[49] H.O. Yazdani, H. Huang, A. Tsung, Autophagy: dual response in the development of hepatocellular carcinoma, Cells 8 (2019) 91, https://doi.org/10.3390/cells8020091.
[50] C. Zhu, M. Zhao, L. Fan, X. Cao, Q. Xia, J. Zhou, H. Yin, L. Zhao, Chitopentaose inhibits hepatocellular carcinoma by inducing mitochondrial mediated apoptosis and suppressing protective autophagy, Bioresour. Bioprocess 8 (2021) 1–12, https://doi.org/10.1186/s40643-020-00358-y.
[51] M. Mostafaei Dehnavi, A. Ebadi, A. Peirovi, G. Taylor, S.A. Salami, THC and CBD fingerprinting of an elite cannabis collection from Iran: quantifying diversity to underpin future cannabis breeding, Plants 11 (2022) 129, https://doi.org/10.3390/plants11010129.
[52] K.J. Livak, T.D. Schmittgen, Analysis of relative gene expression data using real-time quantitative PCR and the 2− ΔΔCT method, Methods 25 (2001) 402–408, https://doi.org/10.1006/meth.2001.1262.
[53] A. Gurib-Fakim, Medicinal plants: traditions of yesterday and drugs of tomorrow, Mol. Asp. Med. 27 (2006) 1–93, https://doi.org/10.1016/j.mam.2005.07.008.
[54] E. Woith, M.F. Melzig, Extracellular vesicles from fresh and dried plants—simultaneous purification and visualization using gel electrophoresis, Int. J. Mol. Sci. 20 (2019) 357, https://doi.org/10.3390/ijms20020357.
[55] Q. Wang, X. Zhuang, J. Mu, Z.-B. Deng, H. Jiang, L. Zhang, X. Xiang, B. Wang, J. Yan, D. Miller, Delivery of therapeutic agents by nanoparticles made of grapefruit-derived lipids, Nat. Commun. 4 (2013) 1–13, https://doi.org/10.1038/ncomms2886.
[56] J. Xiao, S. Feng, X. Wang, K. Long, Y. Luo, Y. Wang, J. Ma, Q. Tang, L. Jin, X. Li, Identification of exosome-like nanoparticle-derived microRNAs from 11 edible fruits and vegetables, PeerJ 6 (2018), e5186, https://doi.org/10.7717/peerj.5186.
[57] X. Li, Z. Liang, J. Du, Z. Wang, S. Mei, Z. Li, Y. Zhao, D. Zhao, Y. Ma, J. Ye, Herbal decoctosome is a novel form of medicine, Sci. China Life Sci. 62 (2019) 333–348, https://doi.org/10.1007/s11427-018-9508-0.
[58] S. Ju, J. Mu, T. Dokland, X. Zhuang, Q. Wang, H. Jiang, X. Xiang, Z.-B. Deng, B. Wang, L. Zhang, Grape exosome-like nanoparticles induce intestinal stem cells and protect mice from DSS-induced colitis, Mol. Ther. 21 (2013) 1345–1357, https://doi.org/10.1038/mt.2013.64.
[59] P. Baldrich, B.D. Rutter, H.Z. Karimi, R. Podicheti, B.C. Meyers, R.W. Innes, Plant extracellular vesicles contain diverse small RNA species and are enriched in 10-to 17-nucleotide "tiny" RNAs, Plant Cell 31 (2019) 315–324, https://doi.org/10.1105/tpc.18.00872.
[60] H.A. Dad, T.-W. Gu, A.-Q. Zhu, L.-Q. Huang, L.-H. Peng, Plant exosome-like nanovesicles: emerging therapeutics and drug delivery nanoplatforms, Mol. Ther. 29 (2021) 13–31, https://doi.org/10.1016/j.ymthe.2020.11.030.
[61] P. Śledziński, J. Zeyland, R. Słomski, A. Nowak, The current state and future perspectives of cannabinoids in cancer biology, Cancer Med. 7 (2018) 765–775, https://doi.org/10.1002/cam4.1312.

[62] S. Lal, A. Shekher, A.S. Narula, H. Abrahamse, S.C. Gupta, Cannabis and its constituents for cancer: history, biogenesis, chemistry and pharmacological activities, Pharmacol. Res. 163 (2020), 105302, https://doi.org/10.1016/j.phrs.2020.105302.
[63] E.S. Seltzer, A.K. Watters, D. MacKenzie, L.M. Granat, D. Zhang, Cannabidiol (CBD) as a promising anti-cancer drug, Cancers 12 (2020) 3203, https://doi.org/10.3390/cancers12113203.
[64] P. Alves, C. Amaral, N. Teixeira, G. Correia-da-Silva, *Cannabis sativa*: much more beyond Δ9-tetrahydrocannabinol, Pharmacol. Res. 157 (2020), 104822, https://doi.org/10.1016/j.phrs.2020.104822.
[65] C. Stanly, M. Moubarak, I. Fiume, L. Turiák, G. Pocsfalvi, Membrane transporters in *citrus clementina* fruit juice-derived nanovesicles, Int. J. Mol. Sci. 20 (2019) 6205, https://doi.org/10.3390/ijms20246205.
[66] G. Pocsfalvi, L. Turiák, A. Ambrosone, P. Del Gaudio, G. Puska, I. Fiume, T. Silvestre, K. Vékey, Protein biocargo of citrus fruit-derived vesicles reveals heterogeneous transport and extracellular vesicle populations, J. Plant Physiol. 229 (2018) 111–121, https://doi.org/10.1016/j.jplph.2018.07.006.
[67] C. Stanly, M. Alfieri, A. Ambrosone, A. Leone, I. Fiume, G. Pocsfalvi, Grapefruit-derived micro and nanovesicles show distinct metabolome profiles and anticancer activities in the A375 human melanoma cell line, Cells 9 (2020) 2722, https://doi.org/10.3390/cells9122722.
[68] Z. Deng, Y. Rong, Y. Teng, J. Mu, X. Zhuang, M. Tseng, A. Samykutty, L. Zhang, J. Yan, D. Miller, Broccoli-derived nanoparticle inhibits mouse colitis by activating dendritic cell AMP-activated protein kinase, Mol. Ther. 25 (2017) 1641–1654, https://doi.org/10.1016/j.ymthe.2017.01.025.
[69] E. Berger, P. Colosetti, A. Jalabert, E. Meugnier, O.P. Wiklander, J. Jouhet, E. Errazurig-Cerda, S. Chanon, D. Gupta, G.J. Rautureau, Use of nanovesicles from orange juice to reverse diet-induced gut modifications in diet-induced obese mice, Mol. Ther. Methods Clin. Dev. 18 (2020) 880–892, https://doi.org/10.1016/j.omtm.2020.08.009.
[70] R.J. McKallip, W. Jia, J. Schlomer, J.W. Warren, P.S. Nagarkatti, M. Nagarkatti, Cannabidiol-induced apoptosis in human leukemia cells: a novel role of cannabidiol in the regulation of *p22phox* and *Nox4* expression, Mol. Pharmacol. 70 (2006) 897–908, https://doi.org/10.1124/mol.106.023937.
[71] S. Pagano, M. Coniglio, C. Valenti, M.I. Federici, G. Lombardo, S. Cianetti, L. Marinucci, Biological effects of cannabidiol on normal human healthy cell populations: systematic review of the literature, Biomed. Pharmacother. 132 (2020), 110728, https://doi.org/10.1016/j.biopha.2020.110728.
[72] J. Iqbal, B.A. Abbasi, T. Mahmood, S. Kanwal, B. Ali, S.A. Shah, A.T. Khalil, Plant-derived anticancer agents: a green anticancer approach, Asian Pac. J. Trop. Biomed. 7 (2017) 1129–1150, https://doi.org/10.1016/j.apjtb.2017.10.016.
[73] M. Sharma, J.B. Hudson, H. Adomat, E. Guns, M.E. Cox, In vitro anticancer activity of plant-derived cannabidiol on prostate cancer cell lines, Pharmacol. Pharm. 5 (2014) 806, https://doi.org/10.4236/pp.2014.58091.
[74] N. Kalenderoglou, T. Macpherson, K.L. Wright, Cannabidiol reduces leukemic cell size–but is it important? Front. Pharmacol. 8 (2017) 144, https://doi.org/10.3389/fphar.2017.00144.
[75] X. Zhang, Y. Qin, Z. Pan, M. Li, X. Liu, X. Chen, G. Qu, L. Zhou, M. Xu, Q. Zheng, Cannabidiol induces cell cycle arrest and cell apoptosis in human gastric cancer SGC-7901 cells, Biomolecules 9 (2019) 302, https://doi.org/10.3390/biom9080302.
[76] G.L. Kelly, A. Strasser, The essential role of evasion from cell death in cancer, Adv. Cancer Res. 111 (2011) 39–96, https://doi.org/10.1016/B978-0-12-385524-4.00002-7.
[77] N.N. Danial, BCL-2 family proteins: critical checkpoints of apoptotic cell death, Clin. Cancer Res. 13 (2007) 7254–7263, https://doi.org/10.1158/1078-0432.CCR-07-1598.
[78] J.E. Chipuk, T. Kuwana, L. Bouchier-Hayes, N.M. Droin, D.D. Newmeyer, M. Schuler, D.R. Green, Direct activation of *Bax* by *p53* mediates mitochondrial membrane permeabilization and apoptosis, Science 303 (2004) 1010–1014, https://doi.org/10.1126/science.1092734.
[79] P. Massi, A. Vaccani, S. Ceruti, A. Colombo, M.P. Abbracchio, D. Parolaro, Antitumor effects of cannabidiol, a nonpsychoactive cannabinoid, on human glioma cell lines, J. Pharmacol. Exp. Ther. 308 (2004) 838–845, https://doi.org/10.1124/jpet.103.061002.
[80] P. Massi, A. Vaccani, S. Bianchessi, B. Costa, P. Macchi, D. Parolaro, The non-psychoactive cannabidiol triggers caspase activation and oxidative stress in human glioma cells, Cell Mol. Life Sci. 63 (2006) 2057–2066, https://doi.org/10.1007/s00018-006-6156-x.
[81] A. Shrivastava, P.M. Kuzontkoski, J.E. Groopman, A. Prasad, Cannabidiol induces programmed cell death in breast cancer cells by coordinating the cross-talk between apoptosis and autophagy, Mol. Cancer Ther. 10 (2011) 1161–1172, https://doi.org/10.1158/1535-7163.MCT-10-1100.
[82] S. Jeong, H.K. Yun, Y.A. Jeong, M.J. Jo, S.H. Kang, J.L. Kim, D.Y. Kim, S.H. Park, B. R. Kim, Y.J. Na, Cannabidiol-induced apoptosis is mediated by activation of *Noxa* in human colorectal cancer cells, Cancer Lett. 447 (2019) 12–23, https://doi.org/10.1016/j.canlet.2019.01.011.